Research Square

Preprints are preliminary reports that have not undergone peer review.
They should not be considered conclusive, used to inform clinical practice,
or referenced by the media as validated information.

Interactome modules underlie shared spatiotemporal patterns in specific psychiatric and neurodegenerative disorders

Kalyani B. Karunakaran

kalyanithepebble@gmail.com

National Institute of Mental Health and Neurosciences

Suhas Ganesh

National Institute of Mental Health and Neurosciences

Jayant Mahadevan

National Institute of Mental Health and Neurosciences

Meera Purushottam

National Institute of Mental Health and Neurosciences

N. Balakrishnan

Indian Institute of Science

Ken-ichi Amemori

Kyoto University

Sanjeev Jain

National Institute of Mental Health and Neurosciences

Biju Viswanath

National Institute of Mental Health and Neurosciences

Article

Keywords: Interactome, transcriptome, genetics, Parkinson's disease, obsessive-compulsive disorder

Posted Date: August 19th, 2026

DOI: https://doi.org/10.21203/rs.3.rs-10583889/v1

License: This work is licensed under a Creative Commons Attribution 4.0 International License.
Read Full License

Additional Declarations: No competing interests reported.

Abstract

Psychiatric and neurological clinical syndromes show considerable overlap, and these have been largely captured by genetic correlation studies. Detailed, hypothesis-generating investigations into the transcriptomic and interactome patterns of risk-related genes, particularly that of their first-order interactors, are lacking. In this study, we examined brain spatiotemporal expression and interactome patterns of risk genes associated with five syndromes with overlapping symptom clusters: obsessive-compulsive disorder (OCD), Huntington's disease (HD), Parkinson's disease (PD), schizophrenia (SZ), and bipolar disorder (BD). The disease gene set, when taken alone, showed no significant interconnectivity in the interactome. However, inclusion of first-order interactors revealed extensive connectivity, exceeding degree-matched random expectations, indicating that the disease genes are embedded within cohesive subnetworks. This enrichment persisted after hub removal, suggesting connectivity is driven by distributed, disease-relevant interactions, rather than global network structure. At the network level, OCD showed a prenatal expression signature with enrichment in foetal structures. Interestingly, the network expression profile of PD, a late-onset syndrome, resembled that of OCD, which presents earlier in life. Further analyses showed that these co-expression signals did not come uniformly from the full syndrome networks, but from groups of highly interconnected proteins that formed specific PD and OCD network modules, and occurred in close proximity in the interactome. They show a prenatal expression signature in the developing prefrontal cortex, and share enrichment for ribosome-related processes. Together, our findings support a network-based model of brain disorders in which genetic risks act through distributed, yet coherent, modules which are organised across brain regions and developmental time periods.

Introduction

Diagnostic algorithms are based on clinical observation, and are the mainstay for differential diagnosis and patient management. However, these disease classifications may not accurately reflect the underlying biological complexity. Clinical syndromes, often assumed to be 'organic' or 'functional' disorders of the brain, overlap considerably as the disease progresses from a prodrome, to a well-defined diagnostic syndrome, over a lifetime. To understand the biological underpinnings of this process, we selected a set of psychiatric and neurodegenerative syndromes that show clinical overlaps. We then jointly studied the transcriptomic and interactome patterns of the risk genes associated with these syndromesto identify shared neurobiological processes.

Obsessive-compulsive disorder (OCD), Huntington's disease (HD), Parkinson's disease (PD), schizophrenia (SZ) and bipolar disorder (BD) manifest compulsive, affective, psychotic, motor, and cognitive symptom clusters. They have overlapping ages of onset, with an early- to mid-life onset for OCD, BD and SZ, and mid-life and late-onset for HD and PD. Obsessions and compulsions are common in both HD and PD,[1, 2] and psychosis and mania may appear in later stages of HD and PD.[3–5] Cognitive decline, and movement abnormalities (including tic disorder), are frequently observed in SZ, BD, and OCD.[6, 7] More generally, comorbid psychiatric and neurodegenerative symptoms are also seen in many

genetic syndromes.[8] The five syndromes likely converge on key neurobiological systems, such as dopaminergic signalling, and striatal circuitry.[9–14] While previous comparisons have examined subsets of these disorders (BD/SZ, PD/SZ, OCD/BD/SZ and PD/BD/SZ),[15–18] a joint analysis of all five – particularly at the transcriptomic and interactome level, would be useful to understand the shared substrate.

The Brainstorm Consortium study (2018) reported a limited overlap across psychiatric and neurological conditions.[17] These correlation estimates may have been sensitive to the power of genome-wide association studies (GWASs) at the time. A recent study by Smeland et al. (2025), however, has demonstrated substantial correlations across the spectrum.[19] These genetic correlation studies have substantially improved our understanding of cross-disorder overlaps and distinctions. To extend these findings and link them to biological mechanisms, detailed, hypothesis-generating investigations of risk variant-harbouring genes are needed. Studying their brain expression signatures and protein-protein interactions (PPIs) can help identify shared or distinct cellular functions underlying disease overlap.

Importantly, a few key transcriptomic and interactome analyses (alongside local genetic correlation studies) have revealed significant cross-disorder overlaps.[20–22] For example, proteins coded by risk genes of psychiatric and neurodegenerative disorders had twice the expected number of PPIs among them.[21] A study from our group identified prenatally-expressed interactome clusters, linking PD and SZ to disrupted neurodevelopment and regeneration.[23] Understanding biological overlaps is also critical for patient care, as the drugs used to manage these conditions may produce adverse effects. In prior work, we identified direct interactions between PD risk-related genes and targets of first-generation antipsychotics causing Parkinsonian side effects.[24]

In this study, we integrate transcriptomic and interactome frameworks to examine OCD, HD, PD, SZ and BD, as being part of a dynamic, comorbid spectrum. Gene expression studies are essential for identifying the neural circuits underlying different syndromes. Earlier studies have linked gene expression to anatomical and functional brain networks.[25–30] However, PPI networks, and their constituent ‘functional units’ (or ‘modules’), have not been connected to spatial expression profiles of specific neural circuits. The human interactome has a modular structure. It is organised into groups of genes that often participate in the same cellular functions, and these modules are highly interconnected within the group, and less connected to genes in other modules.[31, 32]

We investigated the spatiotemporal expression profiles of (I) common variant-harbouring genes associated with OCD, HD, PD, SZ, and BD from the GWAS catalog,[33] then (II) their corresponding syndrome networks and (III) constituent modules, using transcriptomic data from the BrainSpan Atlas[34] and PPI data from BioGRID[35] and HPRD.[36] Fig. 1 shows the overall study design.

Results

Gene compilation

Genes associated with HD, PD, OCD, SZ, and BD were compiled from the GWAS catalog.[33] These genes were located within 50 kb of SNPs with p-values < 10^{-5} (nominal significance), consistent with the threshold applied by GWAS catalog to map genes to SNPs. The total number of genes that emerged varied, with OCD and HD having the least (34 and 59, respectively), while PD has 535, and BD and SZ have 970 and 2,315, respectively. We considered two ways to reduce the number of genes for the latter set of syndromes: (1) only consider "reported genes" from the GWAS catalog (i.e., genes highlighted in the respective publications based on authors' interpretations, biological context, or evidence from functional experiments) and disregard other genes within the 50 kb window, or (2) increase the SNP-level p-value threshold to < 10^{-8} (genome-wide significance). However, both these approaches would severely limit the number of HD and OCD genes.

We therefore filtered the PD-, BD-, and SZ-associated GWAS traits to include loci most likely reflecting high genetic load, namely, positive family history or specific mutation carriers, and core/severe disease symptoms. Therefore, the GWAS traits selected for PD were familial PD, age of onset of PD (age at which PD manifestations first appear), early-onset PD (PD characterised by an age of onset between 21–45 years), motor and cognitive symptoms in PD, and PD in *GBA* mutation carriers (PD with GBA carrier status as the background trait). For SZ, these were early-onset SZ (first onset of schizophrenia before 18 years), age of onset of SZ (age at which SZ manifestations first appear), and treatment-resistant SZ. For BD, these were early-onset BD, age of onset of BD, psychotic symptoms in BD, depressive and manic episodes in BD, and early vs. late onset in BD. For OCD and HD, all available GWAS traits were included. For HD, these were progression of HD and age of onset of HD. For OCD, these were multi-trait GWAS analysis of OCD, various OCD dimensions (aggression, contamination, order, and hoarding), OCD scores (compulsion and obsession), and OCD severity. After applying these filters, we obtained 173 disease associated genes, which included 59 risk genes for HD, 29 for PD, 34 for OCD, 31 for SZ, and 20 for BD (**Supplementary Data File 1**). No overlapping genes were identified across the syndromes.

Spatial expression patterns of syndrome genes and networks

Expression data was available for 115 of the 173 disease-associated genes; these 115 genes include 38 HD, 22 PD, 19 OCD, 21 SZ, and 15 BD genes. We analysed their expression across 26 brain structures using RNA-sequencing data from 42 brains in BrainSpan Atlas.[34] Hierarchical clustering revealed their bifurcation into spatial cluster 1 with 49 genes highly expressed in adult brain structures, and spatial cluster 2 with 66 genes expressed in transitory foetal structures (Fig. 2a). These clusters did not show any statistically significant enrichment for genes linked to a specific syndrome (Fig. 2b). However, a few trends emerged (Fig. 2c): OCD genes were overrepresented in spatial cluster 2 (foetal structures), and risk genes of other syndromes in spatial cluster 1 (adult brain structures).

Since statistically significant enrichment of risk genes was not found in the spatial clusters, we extended the analysis to their first-order interactors in the human interactome. Using PPI data from BioGRID[35] and HPRD,[36] we constructed syndrome-specific networks containing risk genes and their first-order interactors: HD network (488 genes), PD network (857 genes), OCD network (184 genes), SZ network (452 genes), and BD network (217 genes). Of the 2,198 genes across the five networks, 1,595 were uniquely found in one of the five syndrome networks, i.e., HD (342 genes), PD (663 genes), OCD (131 genes), SZ (320 genes) and BD (139 genes), while 267 genes overlapped across two or more syndrome networks (**Supplementary Data File 2**), yielding a total of 1,862 genes for analysis. Interestingly, the combined network of 1,862 genes formed a single connected component (Fig. 3a). This suggests that the risk genes of these syndromes that span the psychiatric-neurodegenerative spectrum are interconnected through first-order interactions.

Notably, the disease gene set alone showed no significant intra-set connectivity in Monte Carlo degree-preserving analyses (Fig. 3b; 22 observed vs. 23.7 ± 4.2 degree-matched random edges; $z = -0.42$, $p = 0.71$; 1,000 iterations). However, including their first-order interactors (1,862 genes) revealed 34,702 intra-set edges, significantly exceeding degree-matched random expectation (Fig. 3c, 33,390 ± 281; $z = 4.67$, $p < 0.001$; 1,000 iterations), indicating that disease genes are embedded within a cohesive subnetwork in the human interactome. To examine whether this enrichment was driven by highly connected hubs, we repeated the analysis after removing the top 1% and 5% of nodes ranked by degree. Enrichment remained significant after hub exclusion: 16,312 observed vs. 14,715 ± 148.6 random edges ($z = 10.7$, $p < 0.001$; 300 iterations) after 1% removal (**Supplementary Fig. 1a**), and 4,942 observed vs. 3,869 ± 56.5 random edges ($z = 19.0$, $p < 0.001$; 300 iterations) after 5% removal (**Supplementary Fig. 1b**). For comparison, the full network yielded 34,702 observed vs. 33,427 ± 308 random edges with 300 iterations ($z = 4.1$, $p < 0.001$) (**Supplementary Fig. 1c**). Hence, enrichment remained robust despite reduced network size and edge count following hub removal. This suggests that connectivity among disease and first-order genes is not hub-dependent.

Figure 3d shows the number of genes co-occurring in multiple syndrome networks, and those unique to each. Overall, each of these networks shared 23%-36% of their genes with any of the four other networks, while 64%-77% of genes were unique to each network (Table 1). Statistical analysis revealed significant interactome overlaps among HD-PD, PD-SZ, and BD-SZ networks (Fig. 3e and Table 2). In comparison, OCD showed overlaps of lower statistical significance. Since HD and PD have monogenic or oligogenic bases identified through family studies, we separately examined the proximity of these genes to the risk genes included in our study. For HD, we selected *HTT*,[37] and for PD, we selected 14 high-confidence genes harbouring PD-linked rare variants, supported by evidence from independent family-based and functional studies.[38] *HTT* was identified as a first-order interactor of the HD-linked gene *SETD2* in our analysis (**Supplementary Fig. 2a**). Among the 14 PD genes, six were present in our PD interactome: *SNCA* as a PD-linked gene itself, *PARK7*, *PINK1*, *LRRK2*, and *GBA* as first-order interactors of *SNCA* (among others), and *ATP13A2* as a first-order interactor of the PD-linked gene *GAK* (**Supplementary Fig. 2b**).

Table 1
Number of genes shared by each syndrome network with any of the four other networks.

Syndrome	# Total genes in syndrome network	# Genes uniquely found in network	% Genes uniquely found in network	% Genes shared with any of the other four networks
Parkinson's disease	857	663	77.4	22.6
Huntington's disease	488	342	70	30
Schizophrenia	452	320	71	29
Bipolar disorder	217	139	64	36
Obsessive-compulsive disorder	184	131	71.2	28.8

Table 2
Number of genes exclusively shared between various pairs of syndrome networks.

Syndrome overlap (Network I - Network II)	Number of genes shared exclusively between Network I and Network II	% of Network I covered by shared genes	% of the Network II covered by shared genes
HD - PD	64	13.1	7.5
PD - SZ	52	6.1	11.5
BD - PD	20	9.2	2.3
OCD - PD	16	8.7	1.9
BD - SZ	15	7	3.3
BD - HD	14	6.4	2.9
HD - OCD	13	2.7	7.1
HD - SZ	12	2.4	2.6
OCD - SZ	7	3.8	1.5
BD - OCD	2	0.9	1.1

Next, we collectively examined the network genes shown in Fig. 3a. Of the 1,862 genes, expression data was available for 1,826 genes. Hierarchical clustering split these into two spatial clusters: spatial cluster 1 with 1,158 genes expressed in foetal structures, and spatial cluster 2 with 668 genes expressed in adult brain structures (Fig. 4a). Spatial cluster 1 showed statistically significant enrichment for the OCD network, and spatial cluster 2 for the HD network (Fig. 4b). Although non-significant, PD network showed an enrichment profile similar to the OCD network, while BD and SZ network enrichments (although non-

significant) resembled the HD network (Fig. 4b). Although the enrichment profiles of the PD, BD and SZ networks were not statistically significant, they suggested patterns, which we explored further by splitting the syndrome networks into modules. Module-level analysis identified specific modules with statistically significant spatial enrichments.

The foetal regions that contributed to spatial cluster 1 included ganglionic eminences and rhombic lip; and hippocampus, mediodorsal nucleus of the thalamus, primary motor cortex, and striatum crossed the significance threshold for spatial cluster 2 (Fig. 4c). The spatial clusters were recapitulated with GTEx data for 12 brain regions (**Supplementary Fig. 3** and **Supplementary Note 1**).

Overall, statistically significant spatial signatures emerged at the level of syndrome networks. We hypothesized that similar enrichment peaks for syndrome networks in specific brain structures may be driven by smaller, tightly linked subnetworks or 'modules' within the networks, and not the entire networks themselves.

Modules within syndrome networks

First, there was no clear indication that syndrome-specific spatial signals came uniformly from the full syndrome networks (**Supplementary Fig. 4** and **Supplementary Note 2**). Next, using methods described by Li et al.[39] and the MCODE algorithm, we asked whether syndrome networks contained modules (defined using multiple parameters; see **Methods**). We confirmed that the syndrome networks have a modular organisation. Thirteen modules were found in the PD network (PD-1 to PD-13), nine each in HD (HD-1 to HD-9) and OCD (OCD-1 to OCD-9) networks, seven in the SZ network (SZ-1 to SZ-7), and six in the BD network (BD-1 to BD-6) (**Supplementary Data File 3**). Five modules – BD-4, HD-7, PD-3, PD-6, and SZ-1 – showed statistically significant enrichment that survived FDR correction (using the Benjamini-Hochberg method) for specific brain structures (**Supplementary Fig. 5**).

In the previous section (Fig. 4), clustering of the network genes revealed two spatial clusters, within which a preferential enrichment of specific syndrome networks was seen. We examined the association of these 44 modules, with the two spatial clusters, to check whether any of them drives the enrichments. Interestingly, specific modules showed enrichments that aligned with the network-level enrichments: OCD-1, PD-3 & PD-4 were enriched in spatial cluster 1, and HD-1, HD-3 & SZ-5 in spatial cluster 2 (Fig. 5a). This suggests that specific modules within network may drive the enrichment patterns seen in Fig. 4.

A microarray dataset with higher sampling resolution from Allen Brain Atlas (covering ~ 230 brain structures) largely recapitulated the cross-disorder relationships at network-level (**Supplementary Note 3**). The BrainSpan clusters were split into specific sub-clusters in this dataset (**Supplementary Figs. 6–8**). However, the network enrichments did not clearly correspond to modules as seen with BrainSpan data (see **Discussion**). Several possibilities can explain this lack of correspondence. The developmental dimension of brain organisation, which influenced the bifurcation of the BrainSpan clusters, is not

captured by the adult microarray dataset. Instead, hierarchical clustering of the latter may have become more sensitive to finer regional specificities. At this higher sampling resolution, the expression patterns of the PPI network modules may have become dispersed across several sub-regions. Technical differences between the RNA-seq and microarray datasets may also contribute. RNA-seq data captures a greater dynamic range of expression values, whereas microarray probe intensity data is more sensitive to signal saturation, and may capture a narrower range of expression.

Functions associated with the modules

Interestingly, OCD-1 occurs proximal to PD-3 & PD-4 (Fig. 5b), and SZ-5 next to HD-1 & HD-3 (Fig. 5c), while maintaining modular separation, and directly interacting with one another. We speculated that this proximity suggested shared underlying mechanisms. Gene Ontology (GO) was used to identify biological processes, cellular components, and molecular functions,[40] enriched across these modules, and KEGG[41] and Reactome,[42] to identify pathways. See **Supplementary Data File 4** for a matrix of function terms (rows) × modules (columns), with each cell containing a $-\log_{10}$(p-value) indicative of the statistical significance of enrichment (threshold set at FDR-adjusted p-value < 0.05, i.e., $-\log_{10}$p-value = 1.3). From this matrix, we identified functions that were significantly enriched either across all co-expressed modules (e.g., OCD-1, PD-3 and PD-4) or across two co-expressed modules from different syndromes (e.g., OCD-1 and PD-3), with the goal of identifying putative common mechanisms across syndromes.

The GO biological process, ribonucleoprotein complex biogenesis, was commonly enriched across OCD-1, PD-3 and PD-4. Between OCD-1 and PD-4, RNA catabolic process was additionally enriched. Across the three modules, metabolism of RNA emerged as a significant Reactome pathway. Ribosome was identified as a significant GO cellular component and KEGG pathway, while structural integrity of the ribosome (annotated in GO as “structural constituent of ribosome”) was identified as a significant GO molecular function.

No GO biological process was commonly enriched across HD-1, HD-3 and SZ-5. Between HD-1 and SZ-5, processes related to protein autophosphorylation, peptidyl-tyrosine modification, immune response-regulating signalling pathway, and T cell activation, were commonly enriched. Between HD-3 and SZ-5, we found enrichment of ribonucleotide metabolic process, nucleotide-excision repair, and nucleoside monophosphate/triphosphate metabolic process.

Since ribosomal processes emerged as a consistent theme across OCD-1, PD-3 and PD-4, we used Monte Carlo analyses to test whether the occurrence of genes associated with the GO term “ribonucleoprotein complex biogenesis” exceeded random expectation for modules of the same size and degree distribution in the human interactome. We found that the number of ribosome-related genes in OCD-1 (5 observed vs. 2 ± 1 genes; $z = 2.64$; $p = 0.027$) and PD-3 (10 observed vs. 4 ± 2 genes; $z = 3.3$; $p = 0.003$) exceeded random expectation. The occurrence of ribosome-related genes in PD-4 was consistent with random expectation (9 observed vs. 8 ± 2 genes; $z = 0.48$; $p = 0.39$). When OCD-1, PD-3 and PD-4

were considered together, the occurrence of 24 ribosome-related genes was non-random (compared to 14 ± 3 genes in random sets; z = 3.18; p = 0.002). In contrast, the number of ribosome-related genes in HD-1 (0 genes observed in module vs. 1 ± 1 genes in degree-matched random sets; z = -1.27; p = 1; 1,000 iterations), HD-3 (2 observed vs. 3 ± 1 genes; z = -0.7; p = 0.85), and SZ-5 (2 observed vs. 3 ± 1 genes; z = -0.7; p = 0.84) was consistent with random expectation. The same held true when HD-1, HD-3 and SZ-5 were considered together (4 observed vs. 7 ± 2 genes; z = -1.44; p = 0.96).

Lastly, we sought to identify the regional and developmental specificities of the six modules. We used a hypergeometric test to examine whether genes highly expressed in a specific brain region and developmental time point, relative to others (from BrainSpan Atlas, computations described by Rouillard et al.[43]), were overrepresented in any of the modules. Genes expressed in the dorsolateral prefrontal cortex at early developmental stages were commonly enriched across OCD-1, PD-3 and PD-4 (Fig. 6a and **Supplementary Data File 5**). In addition, genes expressed in orbital frontal and ventrolateral prefrontal cortices during early stages were enriched in both OCD-1 and PD-4. Between PD-3 and PD-4, common enrichments were observed for the ganglionic eminences, amygdala, hippocampus, anterior cingulate cortex, parietal neocortex, and primary motor-sensory cortex. HD-1 and HD-3 did not show any regional or temporal specificities. SZ-5 showed enrichment for parietal neocortex and hippocampus.

Overall, groups of genes prenatally co-expressed in prefrontal cortical areas likely give rise to modules of interacting proteins participating in ribosome-related processes, and they likely underlie the PD-OCD relationship.

Temporal expression patterns of syndrome genes and networks

Using BrainSpan, we next examined the expression of risk genes and syndrome networks across ten developmental stages (composed of 31 temporal points). In the previous section, we noted a clear correspondence between network and module enrichments in the hierarchically clustered spatial clusters. However, hierarchical clustering of temporal expression profiles did not yield such correspondences (**Supplementary Note 4** and **Supplementary Figs. 9–11**). Time-series clustering that captures smooth developmental trajectories revealed clearer module-to-network matches than hierarchical clustering, e.g., OCD and SZ module enriched in clusters peaking at specific stages (**Supplementary Note 4** and **Supplementary Fig. 12**). This suggested that these syndrome-specific modules are perhaps dynamically expressed over development. However, we did not note any co-enrichment of modules from different syndrome networks in these clusters.

Discussion

Key findings on cross-disorder overlaps have largely come from genetic correlation studies. Systematic hypothesis-generating investigations into the transcriptomic and interactome patterns of risk-related genes, particularly that of their first-order interactors, are lacking. To address this gap, we compared the spatiotemporal expression profiles of risk genes linked to five syndromes spanning the psychiatric-

neurodegenerative spectrum, and their interactomes. Three key findings emerged: (I) The risk genes were connected through first-order interactions. (II) Statistically significant disease-linked spatial signals co-emerged at the network level, and proximally occurring modules (groups of highly interconnected genes) within syndrome networks, rather than the entire networks, drove these cross-disorder patterns. These co-enriched modules also shared functions, suggesting a mechanistic basis for the observed co-expression patterns. (III) PD- and OCD-related network expression signals emerged together, and we identified prenatally-expressed PD and OCD modules involved in ribosome-related processes.

Risk genes were connected through first-order interactions

We observed that the disease genes did not form a highly connected network on their own, but lay within a broader neighbourhood of strongly interconnected first-order interactors. The persistence of enrichment after removing the top 1% and 5% of hubs suggests that this pattern is driven more by distributed, disease-relevant interactions, rather than by the global network structure. This supports the view that disease biology arises from perturbations within local subnetworks, rather than isolated genes. Prior work has shown a significant enrichment for PPIs among 118 proteins linked to psychiatric and neurodegenerative conditions, including PD, BD and SZ. Our results extend these findings and show that modules within the broader interactome likely drive the shared spatiotemporal expression patterns of psychiatric and neurological syndromes, cutting across their diagnostic boundaries.

Cross-disorder expression signatures were driven by proximal modules

Functional association networks integrating PPIs, co-expression, and other associations have been used for network-based stratification of disease subtypes.[44] However, PPI networks, comprising experimentally verified protein interactions, have not been systematically linked to spatial expression profiles reflecting neural circuits. Earlier studies have linked gene expression to anatomical and functional brain networks.[25–30] Studies from our group and others[39, 45–50] consistently report syndrome-linked brain-expressed genes self-organizing into clusters based on similar spatial expression profiles, often reflecting anatomical and functional connectivity. Extending this, and well-established concepts of PPI modularity and disease-associated modules,[51, 52] we link PPI networks and modules to regional expression patterns. Importantly, the modules enriched in spatial clusters were selectively derived from syndrome networks that themselves showed enrichment. This suggested that these modules are perhaps “responsible” for the observed signals. Modules co-enriched in the spatial clusters were part of related GO processes, perhaps, because (genes coding for) proteins with concerted cellular functions in the same brain region are likely to co-express. Similar expression signals may emerge for multiple syndromes, because proteins occupy proximate neighbourhoods in the interactome.

In our current analyses, we retained both spatial and temporal dimensions, but examined them separately by using only the spatial (or temporal) labels to organize the X-axis and performing

hierarchical clustering along the gene (Y) axis. This approach was adopted to identify spatially- and temporally- defined gene clusters for downstream analysis and ease of analysis and interpretation. While with regional specificities, across syndromes, we could detect specific groups of co-expressed genes that formed PPI modules participating in similar functions, we were not able to identify such modules with temporal expression profiles. Perhaps, this indicates that broad developmentally regulated patterns, without incorporating regional specificities, do not map as clearly to PPI networks and modules as region-specific profiles. However, spatially co-occurring modules were enriched for specific developmental stages. This suggests that syndrome network signals co-emerged when development signals were captured in tandem with regional specificities. Hence, both the spatial and temporal axes are required to understand cross-disorder dynamics.

Prenatally-expressed PD and OCD modules likely involved in ribosome-related processes

Simple computation of gene overlaps between syndrome networks revealed links between HD-PD, PD-SZ and BD-SZ (Fig. 3c). The HD-PD overlap likely reflects shared cellular processes reflective of clinical semiology.[53] Shared connection to dopaminergic signalling and symptom overlap in conditions like Lewy body dementia and 22q11 deletion syndrome may be reflected in the PD-SZ overlap.[54–58] The BD-SZ overlap may reflect shared genetic risk and symptoms, and familial co-aggregation.[59–61] OCD showed the least overlap with other syndromes, suggesting somewhat distinct mechanisms. However, expression-based clustering of the network genes provided a more detailed picture.

Spatial clustering of network genes showed that multiple syndromes shared similar regional profiles (e.g., OCD and PD). The OCD network showed a foetal signature involving several prenatal structures. Time-series analysis also showed that OCD had a prenatal bias. Rodent models of OCD-related behaviours involve knockouts of genes encoding proteins critical for neurodevelopment and neurotransmitter function (e.g., *Sapap3*, *Slitrk5, Hoxb8*).[62] In targeted gene sequencing studies, variations in the *SAPAP3* gene have been associated with early-onset OCD.[63] OCD has also been linked to prenatal and perinatal complications,[64–67] and this supports the conjecture that early developmental disruptions contribute to the syndrome. Interestingly, although non-significant, the network expression profile of PD, emerging later in life, resembled that of OCD, which emerges earlier in life. A few transcriptome- and network-based studies have reported a prenatal expression signature and neurodevelopmental involvement for specific PD-related risk genes,[68, 69] although deeper investigations are lacking.

The evidence for the presence of OC symptoms in PD is conflicting. A few studies report a higher incidence of OC symptoms in PD and attribute this to the involvement of frontal-basal ganglia circuitry in both syndromes.[70, 71] Another study reports no significant differences in the incidence of clinical and subclinical OCD, or in the type and severity of OC symptoms, in idiopathic PD patients and matched medically ill controls.[71] A more recent study showed that OCD patients have a substantially higher risk of developing PD, with the risk magnified for patients with a higher number of psychiatric outpatient

visits.[72] Interestingly, a significant association has been reported between PARKIN mutation status and OC symptom levels in early-onset PD patients and their asymptomatic relatives.[73] Specifically, PARKIN carrier patients showed fewer OC symptoms than non-carriers, whereas PARKIN carrier asymptomatic relatives showed more OC symptoms than non-carriers. These findings suggest a complex relationship between PD genetics and OC symptoms.

Our study finds indications of a PD-OCD relationship along three axes: (1) specific PD and OCD modules occur in close proximity in the interactome; (2) they show a prenatal expression signature in the developing prefrontal cortex across the syndrome modules (and in the ganglionic eminences for the PD modules); and (3) they share a ribosome-related signal. Broadly, these observations lead one to speculate that perturbations in ribosomal genes during neurodevelopment could modify susceptibility to both OCD and PD. Within the scope of the current study, note that this is proposed as a testable hypothesis, and not as a definitive mechanism. This hypothesis can be examined in OCD- and PD-patient-derived induced pluripotent stem cell (IPSC) lines, an important ongoing line of enquiry in our group.

Previous studies have reported differential expression of genes encoding ribosomal proteins in peripheral blood of OCD patients and in the frontal cortex (and other regions) of PD patients.[74, 75] *LRRK2* is an important PD risk-related gene. The protein interacts with several ribosomal proteins, and is involved in ribosomal function and mRNA translation.[76] It has been shown that blocking ribosomal protein s15 phosphorylation rescues mutant LRRK2-mediated neurotoxicity in human midbrain dopamine neurons and cortical neurons.

To examine the scope of our hypothesis, we systematically assessed whether the 24 ribosome-related genes identified in the OCD-1, PD-3 and PD-4 modules (Fig. 6b) were differentially expressed in publicly available OCD and PD postmortem brain datasets (fold change > 1.2 for overexpression or < $\raisebox{1ex}{\$1\$}/\raisebox{-1ex}{\$1.2\$}$ for underexpression; p-value < 0.05). Using BaseSpace Correlation Engine,[77] we collected four OCD-associated differential gene expression (DGE) datasets from prefrontal cortex and caudate nucleus, and 45 PD datasets from frontal cortical regions, multiple subcortical regions, and the cerebellum (**Supplementary Data File 6**). Nineteen of the 24 genes were differentially expressed in at least one OCD dataset and at least one PD dataset (Fig. 6c and **Supplementary Data File 6**); four of these appeared in both the OCD datasets and in at least two PD datasets (Fig. 6d and **Supplementary Data File 6**). Seven ribosome-related genes were identified in the single frontal cortical OCD dataset available to us and in at least one of the four frontal cortical PD datasets (Fig. 6e and **Supplementary Data File 6**); this overlap was computed given the frontal cortical signature identified for these modules.

Limitations of the study

Our study has several limitations. Cross-disorder overlaps were interpreted based on shared neural signatures; assessment of large-scale patient data is additionally required to determine whether these

reflect comorbidity or shared clinical features. Additionally, these overlaps are contextual, limited by the specific set of syndromes examined. We will analyse the interactomes and transcriptomes of an expanded syndrome set in a future study. While we incorporated spatiotemporal expression data, the interactome model remains static, limiting its ability to capture the multifactorial aetiology of these syndromes. Still, it provides a systematic framework for transdiagnostic analysis.

Conclusions

Together, our findings support a network-based model of brain disorders in which genetic risk acts through distributed, but coherent, modules. Disease-relevant proteins are organised into local subnetworks and they likely shape the formation and functioning of circuits. Perturbations within these modules may bias neural systems toward disease vulnerability, before symptoms begin, or pathology is detected. The overlapping molecular networks and the cellular functions they regulate, could account for particular symptom clusters occurring withing the defined syndromes. We show that transcriptome- and interactome-based studies help capture themes shared across diagnostic boundaries and generate testable hypotheses on cross-disorder overlaps.

Methods

Compilation of disease risk genes

Genes harbouring variants associated with the five syndromes were compiled from the GWAS catalog,[33] namely, 59 for HD, 29 for PD, 34 for OCD, 31 for SZ, and 20 for BD (**Supplementary Data File 1**). PD-, BD-, and SZ-associated GWAS traits were filtered to retain loci most likely reflecting a high genetic load, to address disparities in the number of genes linked with each syndrome.

Syndrome network construction and module identification

The PPI repositories BioGRID[35] (version 4.3.194) and HPRD[36] (version 9) were used to compile the first-order PPIs. Specifically, direct interactions (MI:0407) and physical associations (MI:0915) of the proteins encoded b the disease-linked genes were compiled, and HD, PD, OCD, SZ and BD interactomes were constructed (**Supplementary Data File 2** and **Supplementary Methods 1**). Following methods described by Li et al.,[39] we decomposed these syndrome networks into 44 topological modules using the Cytoscape plugin MCODE (**Supplementary Data File 3** and **Supplementary Methods 2**).[78] Cytoscape was used to visualise the networks and the modules.[79]

Degree-preserving network analyses

We examined whether disease genes form a connectivity-enriched subnetwork using a degree-preserving empirical test. For each of 1,000 iterations, we generated a comparison set by sampling nodes from the interactome such that the sampled nodes matched the degree of each disease gene (± 1). For every random set, we counted the number of intra-set edges. This generated a null distribution of degree-matched networks against which we compared the observed value. Enrichment was quantified using the empirical p-value and z-score from the null distribution. We repeated the analysis with an expanded set comprising disease genes and their first-order interactors (comparison with 1,000 random sets). To test robustness of this expanded set to hub structure, we re-ran the same degree-matched procedure by removing the (i) top 1% and (ii) top 5% highest-degree nodes from the interactome and (iii) without removing any hubs (comparison with 300 random sets).

Hierarchical clustering and time-series analyses of expression profiles

We analysed RNA-sequencing data from human brains in BrainSpan Atlas[34] to identify syndrome gene and network clusters with distinct spatial and temporal expression profiles (see **Supplementary Methods 3** for data description). The dataset included 524 samples across 31 temporal points. For independent replication of the spatial results, we used GTEx RNA-seq data.[80] To identify the regional specificities of the spatial clusters, we used microarray data comprising 3,702 samples from Allen Brain Atlas.[81] Average probe intensity or RPKM values were $\log_2$-transformed, and hierarchical clustering was performed using Morpheus software (**Supplementary Methods 4**).[82] Pairwise distances were calculated using Pearson correlation, and clusters were identified using the average linkage method. Enrichment analysis of spatial clusters for genes highly expressed in specific structures was performed using hypergeometric tests, with correction for multiple hypotheses applied using the Benjamini-Hochberg (BH) method (**Supplementary Methods 5**). Mfuzz time-series analysis, a soft clustering method, was performed to measure the extent to which syndrome network genes follow a predominant clustering pattern based on their expression changes across the different developmental stages.[83]

Functional enrichment analyses

Functional enrichment of clusters for biological processes (Gene Ontology[40]) was computed using WebGestalt,[84] with statistical significance assessed via the hypergeometric test and corrected for multiple hypotheses using the BH method (**Supplementary Methods 6**).

Declarations

Competing Interests:

None.

Funding:

This work was supported by the Centre for Brain and Mind (G-202303-00523 to K.B.K, J.M, M.P, and B.V), MQ: Transforming Mental Health Fellowship (MQF22/20 to S.G), SKAN Research Trust (SKAN/002/208/2021/01481 to K.B.K, M.P, B.V and S.J), DBT/Wellcome Intermediate Fellowship (IA/CPHI/20/1/505266 to B.V), MEXT/JSPS KAKENHI Grants (JP25K02377, JP22H04998, JP24H02163 to K.A), and AMED Grants (JP24gm6910012, JP24wm0625210 to K.A). S.J acknowledges the Department of Biotechnology (Government of India) grant entitled “Accelerator program for discovery in brain disorders using stem cells” (ADBS) for funding (BT/PR17316/MED/31/326/2015).

Author Contribution

K.B.K, S.J and B.V conceived the project. K.B.K collected the datasets, designed the methodology and performed the analyses. B.V, S.J, K.A, M.P, S.G, J.M and N.B helped refine the work through iterative feedback. K.B.K wrote the manuscript. All authors edited and approved the manuscript.

Acknowledgement

The authors thank Mythri S.V (NIMHANS) for helpful suggestions on the work.

Data Availability

The disease risk-related genes, interactomes and modules analysed in this study have been made available as Supplementary Data File 1, Supplementary Data File 2 and Supplementary Data File 3, respectively.

References

1. Molano-Eslava JC, Iragorri-Cucalón Á, Ucrós-Rodríguez G, Bonilla-Jácome C, Tovar-Perdomo S, Herin DV, Orozco-Cabal L. Obsessive-compulsive disorder symptoms in Huntington’s disease: a case report. *Revista colombiana de psiquiatria* 2008; 37(4): 644.
2. Monaco MRL, Di Stasio E, Zuccala G, Petracca M, Genovese D, Fusco D *et al.* Prevalence of obsessive-compulsive symptoms in elderly Parkinson disease patients: a case-control study. *The American Journal of Geriatric Psychiatry* 2020; 28(2): 167–175.
3. Taddei RN, Cankaya S, Dhaliwal S, Chaudhuri KR. Management of psychosis in Parkinson’s disease: emphasizing clinical subtypes and pathophysiological mechanisms of the condition. *Parkinson’s Disease* 2017; 2017(1): 3256542.
4. Rosenblatt A, Leroi I. Neuropsychiatry of Huntington’s disease and other basal ganglia disorders. *Psychosomatics* 2000; 41(1): 24–30.

5. Jerčić KG, Blažeković A, Borovečki S, Borovečki F. Non-motor symptoms of Parkinsons disease-insights from genetics. *Journal of Neural Transmission* 2024: 1–8.
6. Stevenson-Hoare J, Legge SE, Simmonds E, Han J, Owen MJ, O'Donovan M *et al.* Severe psychiatric disorders are associated with increased risk of dementia. *BMJ Ment Health* 2024; 27(1).
7. Lombroso PJ, Scahill L. Tourette syndrome and obsessive–compulsive disorder. *Brain and Development* 2008; 30(4): 231–237.
8. Peall KJ, Owen MJ, Hall J. Rare genetic brain disorders with overlapping neurological and psychiatric phenotypes. *Nature Reviews Neurology* 2024; 20(1): 7–21.
9. Obeso JA, Rodriguez-Oroz MC, Stamelou M, Bhatia KP, Burn DJ. The expanding universe of disorders of the basal ganglia. *The Lancet* 2014; 384(9942): 523–531.
10. Macpherson T, Hikida T. Role of basal ganglia neurocircuitry in the pathology of psychiatric disorders. *Psychiatry and clinical neurosciences* 2019; 73(6): 289–301.
11. Johnson CP, Christensen GE, Fiedorowicz JG, Mani M, Shaffer Jr JJ, Magnotta VA, Wemmie JA. Alterations of the cerebellum and basal ganglia in bipolar disorder mood states detected by quantitative T1ρ mapping. *Bipolar disorders* 2018; 20(4): 381–390.
12. Girault J-A, Greengard P. The neurobiology of dopamine signaling. *Archives of neurology* 2004; 61(5): 641–644.
13. Ashok AH, Marques TR, Jauhar S, Nour MM, Goodwin GM, Young AH, Howes OD. The dopamine hypothesis of bipolar affective disorder: the state of the art and implications for treatment. *Molecular psychiatry* 2017; 22(5): 666–679.
14. Cepeda C, Murphy KP, Parent M, Levine MS. The role of dopamine in Huntington's disease. *Progress in brain research* 2014; 211: 235–254.
15. Consortium C-DGotPG. Identification of risk loci with shared effects on five major psychiatric disorders: a genome-wide analysis. *The Lancet* 2013; 381(9875): 1371–1379.
16. Lee PH, Anttila V, Won H, Feng Y-CA, Rosenthal J, Zhu Z *et al.* Genomic relationships, novel loci, and pleiotropic mechanisms across eight psychiatric disorders. *Cell* 2019; 179(7): 1469–1482. e1411.
17. Anttila V, Bulik-Sullivan B, Finucane H, Walters R, Bras J, Duncan L. & Neale, BM (2018). Analysis of shared heritability in common disorders of the brain. *Science*; 360: 6395.
18. Smeland OB, Shadrin A, Bahrami S, Broce I, Tesli M, Frei O *et al.* Genome-wide association analysis of Parkinson's disease and schizophrenia reveals shared genetic architecture and identifies novel risk loci. *Biological psychiatry* 2021; 89(3): 227–235.
19. Smeland OB, Kutrolli G, Bahrami S, Fominykh V, Parker N, Fuhrer J *et al.* A genome-wide analysis of the shared genetic risk architecture of complex neurological and psychiatric disorders. *Nature Neuroscience* 2025: 1–12.
20. Reynolds RH, Wagen AZ, Lona-Durazo F, Scholz SW, Shoai M, Hardy J *et al.* Local genetic correlations exist among neurodegenerative and neuropsychiatric diseases. *npj Parkinson's Disease* 2023; 9(1): 70.

21. Wingo TS, Liu Y, Gerasimov ES, Vattathil SM, Wynne ME, Liu J *et al.* Shared mechanisms across the major psychiatric and neurodegenerative diseases. *Nature communications* 2022; 13(1): 4314.
22. Haglund A, Zuber V, Abouzeid M, Yang Y, Ko JH, Wiemann L *et al.* Cell state-dependent allelic effects and contextual Mendelian randomization analysis for human brain phenotypes. *Nature Genetics* 2025.
23. Karunakaran KB, Jain S, Brahmachari SK, Balakrishnan N, Ganapathiraju MK. Parkinson's disease and schizophrenia interactomes contain temporally distinct gene clusters underlying comorbid mechanisms and unique disease processes. *Schizophrenia* 2024; 10(1): 26.
24. Karunakaran KB, Jain S, Widera D, Cottrell GS. Spatial and functional profiles distinguish target sets of Parkinson's disease and antipsychotic drugs with different clinical effects. *Translational Psychiatry* 2025; 15(1): 124.
25. Anderson KM, Krienen FM, Choi EY, Reinen JM, Yeo BT, Holmes AJ. Gene expression links functional networks across cortex and striatum. *Nature communications* 2018; 9(1): 1–14.
26. Richiardi J, Altmann A, Milazzo A-C, Chang C, Chakravarty MM, Banaschewski T *et al.* Correlated gene expression supports synchronous activity in brain networks. *Science* 2015; 348(6240): 1241–1244.
27. Wang G-Z, Belgard TG, Mao D, Chen L, Berto S, Preuss TM *et al.* Correspondence between resting-state activity and brain gene expression. *Neuron* 2015; 88(4): 659–666.
28. Krienen FM, Yeo BT, Ge T, Buckner RL, Sherwood CC. Transcriptional profiles of supragranular-enriched genes associate with corticocortical network architecture in the human brain. *Proceedings of the National Academy of Sciences* 2016; 113(4): E469-E478.
29. Patania A, Selvaggi P, Veronese M, Dipasquale O, Expert P, Petri G. Topological gene expression networks recapitulate brain anatomy and function. *Network Neuroscience* 2019; 3(3): 744–762.
30. Mills BD, Grayson DS, Shunmugavel A, Miranda-Dominguez O, Feczko E, Earl E *et al.* Correlated gene expression and anatomical communication support synchronized brain activity in the mouse functional connectome. *Journal of Neuroscience* 2018; 38(25): 5774–5787.
31. Barabási A-L, Gulbahce N, Loscalzo J. Network medicine: a network-based approach to human disease. *Nature reviews genetics* 2011; 12(1): 56–68.
32. Barabasi A-L, Oltvai ZN. Network biology: understanding the cell's functional organization. *Nature reviews genetics* 2004; 5(2): 101–113.
33. Buniello A, MacArthur JAL, Cerezo M, Harris LW, Hayhurst J, Malangone C *et al.* The NHGRI-EBI GWAS Catalog of published genome-wide association studies, targeted arrays and summary statistics 2019. *Nucleic acids research* 2019; 47(D1): D1005-D1012.
34. Sunkin SM, Ng L, Lau C, Dolbeare T, Gilbert TL, Thompson CL *et al.* Allen Brain Atlas: an integrated spatio-temporal portal for exploring the central nervous system. *Nucleic acids research* 2012; 41(D1): D996-D1008.
35. Stark C, Breitkreutz B-J, Reguly T, Boucher L, Breitkreutz A, Tyers M. BioGRID: a general repository for interaction datasets. *Nucleic acids research* 2006; 34(suppl_1): D535-D539.

36. Keshava Prasad T, Goel R, Kandasamy K, Keerthikumar S, Kumar S, Mathivanan S *et al.* Human protein reference database—2009 update. *Nucleic acids research* 2009; 37(suppl_1): D767-D772.
37. Bates GP, Dorsey R, Gusella JF, Hayden MR, Kay C, Leavitt BR *et al.* Huntington disease. *Nature reviews Disease primers* 2015; 1(1): 1–21.
38. Blauwendraat C, Nalls MA, Singleton AB. The genetic architecture of Parkinson's disease. *The Lancet Neurology* 2020; 19(2): 170–178.
39. Li J, Shi M, Ma Z, Zhao S, Euskirchen G, Ziskin J *et al.* Integrated systems analysis reveals a molecular network underlying autism spectrum disorders. *Molecular systems biology* 2014; 10(12): 774.
40. Consortium GO. The gene ontology resource: 20 years and still GOing strong. *Nucleic acids research* 2019; 47(D1): D330-D338.
41. Kanehisa M, Araki M, Goto S, Hattori M, Hirakawa M, Itoh M *et al.* KEGG for linking genomes to life and the environment. *Nucleic acids research* 2007; 36(suppl_1): D480-D484.
42. Milacic M, Beavers D, Conley P, Gong C, Gillespie M, Griss J *et al.* The reactome pathway knowledgebase 2024. *Nucleic acids research* 2024; 52(D1): D672-D678.
43. Rouillard AD, Gundersen GW, Fernandez NF, Wang Z, Monteiro CD, McDermott MG, Ma'ayan A. The harmonizome: a collection of processed datasets gathered to serve and mine knowledge about genes and proteins. *Database* 2016; 2016.
44. Chang Y, Glass K, Liu Y-Y, Silverman EK, Crapo JD, Tal-Singer R *et al.* COPD subtypes identified by network-based clustering of blood gene expression. *Genomics* 2016; 107(2–3): 51–58.
45. Karunakaran KB, Amemori K-i. Spatiotemporal expression patterns of anxiety disorder-associated genes. *Translational Psychiatry* 2023; 13(1): 385.
46. Eising E, Huisman SM, Mahfouz A, Vijfhuizen LS, Anttila V, Winsvold BS *et al.* Gene co-expression analysis identifies brain regions and cell types involved in migraine pathophysiology: a GWAS-based study using the Allen Human Brain Atlas. *Human genetics* 2016; 135(4): 425–439.
47. Krishnan A, Zhang R, Yao V, Theesfeld CL, Wong AK, Tadych A *et al.* Genome-wide prediction and functional characterization of the genetic basis of autism spectrum disorder. *Nature neuroscience* 2016; 19(11): 1454–1462.
48. Luo Y, Eran A, Palmer N, Avillach P, Levy-Moonshine A, Szolovits P, Kohane IS. A multidimensional precision medicine approach identifies an autism subtype characterized by dyslipidemia. *Nature Medicine* 2020; 26(9): 1375–1379.
49. Huckins LM, Dobbyn A, Ruderfer DM, Hoffman G, Wang W, Pardinas AF *et al.* Gene expression imputation across multiple brain regions provides insights into schizophrenia risk. *Nature genetics* 2019; 51(4): 659–674.
50. Karunakaran K, Ganesh S, Vishwanath B, Purushottam M, Jain S. Temporal expression signatures of rare variant-harboring genes linked to autism, bipolar disorder, schizophrenia and epilepsy across neurodevelopment. 2025.

51. Buphamalai P, Kokotovic T, Nagy V, Menche J. Network analysis reveals rare disease signatures across multiple levels of biological organization. *Nature communications* 2021; 12(1): 6306.
52. Ghiassian SD, Menche J, Barabási A-L. A DIseAse MOdule Detection (DIAMOnD) algorithm derived from a systematic analysis of connectivity patterns of disease proteins in the human interactome. *PLoS computational biology* 2015; 11(4): e1004120.
53. Gadhave DG, Sugandhi VV, Jha SK, Nangare SN, Gupta G, Singh SK *et al.* Neurodegenerative disorders: Mechanisms of degeneration and therapeutic approaches with their clinical relevance. *Ageing research reviews* 2024: 102357.
54. Walker Z, Possin KL, Boeve BF, Aarsland D. Lewy body dementias. *The Lancet* 2015; 386(10004): 1683–1697.
55. Psychosis in Dementia With Lewy Bodies. *Proceedings of the Seminars in clinical neuropsychiatry*1998.
56. Naimark D, Jackson E, Rockwell E, Jeste DV. Psychotic symptoms in Parkinson's disease patients with dementia. *Journal of the American Geriatrics Society* 1996; 44(3): 296–299.
57. Nalls MA, Pankratz N, Lill CM, Do CB, Hernandez DG, Saad M *et al.* Large-scale meta-analysis of genome-wide association data identifies six new risk loci for Parkinson's disease. *Nature genetics* 2014; 46(9): 989–993.
58. Kobrynski LJ, Sullivan KE. Velocardiofacial syndrome, DiGeorge syndrome: the chromosome 22q11. 2 deletion syndromes. *The Lancet* 2007; 370(9596): 1443–1452.
59. Yamada Y, Matsumoto M, Iijima K, Sumiyoshi T. Specificity and continuity of schizophrenia and bipolar disorder: relation to biomarkers. *Current pharmaceutical design* 2020; 26(2): 191–200.
60. Anttila V, Bulik-Sullivan B, Finucane HK, Walters RK, Bras J, Duncan L *et al.* Analysis of shared heritability in common disorders of the brain. *Science* 2018; 360(6395).
61. Gandal MJ, Haney JR, Parikshak NN, Leppa V, Ramaswami G, Hartl C *et al.* Shared molecular neuropathology across major psychiatric disorders parallels polygenic overlap. *Science* 2018; 359(6376): 693–697.
62. Zhang Y-D, Shi D-D, Wang Z. Neurobiology of obsessive–compulsive disorder from genes to circuits: Insights from animal models. *Neuroscience Bulletin* 2024; 40(12): 1975–1994.
63. Boardman L, van der Merwe L, Lochner C, Kinnear CJ, Seedat S, Stein DJ *et al.* Investigating SAPAP3 variants in the etiology of obsessive-compulsive disorder and trichotillomania in the South African white population. *Comprehensive psychiatry* 2011; 52(2): 181–187.
64. Vasconcelos MS, Sampaio AS, Hounie AG, Akkerman F, Curi M, Lopes AC, Miguel EC. Prenatal, perinatal, and postnatal risk factors in obsessive–compulsive disorder. *Biological Psychiatry* 2007; 61(3): 301–307.
65. Grisham J, Fullana M, Mataix-Cols D, Moffitt T, Caspi A, Poulton R. Risk factors prospectively associated with adult obsessive–compulsive symptom dimensions and obsessive–compulsive disorder. *Psychological medicine* 2011; 41(12): 2495–2506.

66. Brander G, Rydell M, Kuja-Halkola R, de la Cruz LF, Lichtenstein P, Serlachius E *et al.* Association of perinatal risk factors with obsessive-compulsive disorder: a population-based birth cohort, sibling control study. *JAMA psychiatry* 2016; 73(11): 1135–1144.
67. Abdulkadir M, Tischfield JA, King RA, Fernandez TV, Brown LW, Cheon K-A *et al.* Pre-and perinatal complications in relation to Tourette syndrome and co-occurring obsessive-compulsive disorder and attention-deficit/hyperactivity disorder. *Journal of psychiatric research* 2016; 82: 126–135.
68. Li B, Zhao G, Li K, Wang Z, Fang Z, Wang X *et al.* Characterizing the expression patterns of Parkinson's disease associated genes. *Frontiers in Neuroscience* 2021; 15: 629156.
69. Hu Y, Pan Z, Hu Y, Zhang L, Wang J. Network and pathway-based analyses of genes associated with Parkinson's disease. *Molecular neurobiology* 2017; 54(6): 4452–4465.
70. Alegret M, Junque C, Valldeoriola F, Vendrell P, Marti M, Tolosa E. Obsessive-compulsive symptoms in Parkinson's disease. *Journal of Neurology, Neurosurgery & Psychiatry* 2001; 70(3): 394–396.
71. Harbishettar V, Pal PK, Reddy YJ, Thennarasu K. Is there a relationship between Parkinson's disease and obsessive-compulsive disorder? *Parkinsonism & related disorders* 2005; 11(2): 85–88.
72. Liou Y-J, Bai Y-M, Chen M-H, Cheng C-M, Chen T-J, Tsai S-J. Obsessive-compulsive disorder and risk of Parkinson disease: a nationwide longitudinal study. *Biopsychosocial Science and Medicine* 2022; 84(9): 1096–1102.
73. Sharp ME, Caccappolo E, Mejia-Santana H, Tang MX, Rosado L, Orbe Reilly M *et al.* The relationship between obsessive-compulsive symptoms and PARKIN genotype: the CORE-PD study. *Movement Disorders* 2015; 30(2): 278–283.
74. Garcia-Esparcia P, Hernández-Ortega K, Koneti A, Gil L, Delgado-Morales R, Castaño E *et al.* Altered machinery of protein synthesis is region-and stage-dependent and is associated with α-synuclein oligomers in Parkinson's disease. *Acta neuropathologica communications* 2015; 3(1): 76.
75. Song Y, Liu Y, Wu P, Zhang F, Wang G. Genome-wide mRNA expression analysis of peripheral blood from patients with obsessive-compulsive disorder. *Scientific Reports* 2018; 8(1): 12583.
76. Martin I, Kim JW, Lee BD, Kang HC, Xu J-C, Jia H *et al.* Ribosomal protein s15 phosphorylation mediates LRRK2 neurodegeneration in Parkinson's disease. *Cell* 2014; 157(2): 472–485.
77. Kupershmidt I, Su QJ, Grewal A, Sundaresh S, Halperin I, Flynn J *et al.* Ontology-based meta-analysis of global collections of high-throughput public data. *PloS one* 2010; 5(9): e13066.
78. Bader GD, Hogue CW. An automated method for finding molecular complexes in large protein interaction networks. *BMC bioinformatics* 2003; 4(1): 1–27.
79. Smoot ME, Ono K, Ruscheinski J, Wang P-L, Ideker T. Cytoscape 2.8: new features for data integration and network visualization. *Bioinformatics* 2011; 27(3): 431–432.
80. Consortium G. The Genotype-Tissue Expression (GTEx) pilot analysis: Multitissue gene regulation in humans. *Science* 2015; 348(6235): 648–660.
81. Hawrylycz MJ, Lein ES, Guillozet-Bongaarts AL, Shen EH, Ng L, Miller JA *et al.* An anatomically comprehensive atlas of the adult human brain transcriptome. *Nature* 2012; 489(7416): 391.

82. Starruß J, De Back W, Brusch L, Deutsch A. Morpheus: a user-friendly modeling environment for multiscale and multicellular systems biology. *Bioinformatics* 2014; 30(9): 1331–1332.

83. Kumar L, Futschik ME. Mfuzz: a software package for soft clustering of microarray data. *Bioinformation* 2007; 2(1): 5.

84. Liao Y, Wang J, Jaehnig EJ, Shi Z, Zhang B. WebGestalt 2019: gene set analysis toolkit with revamped UIs and APIs. *Nucleic acids research* 2019.

Figures

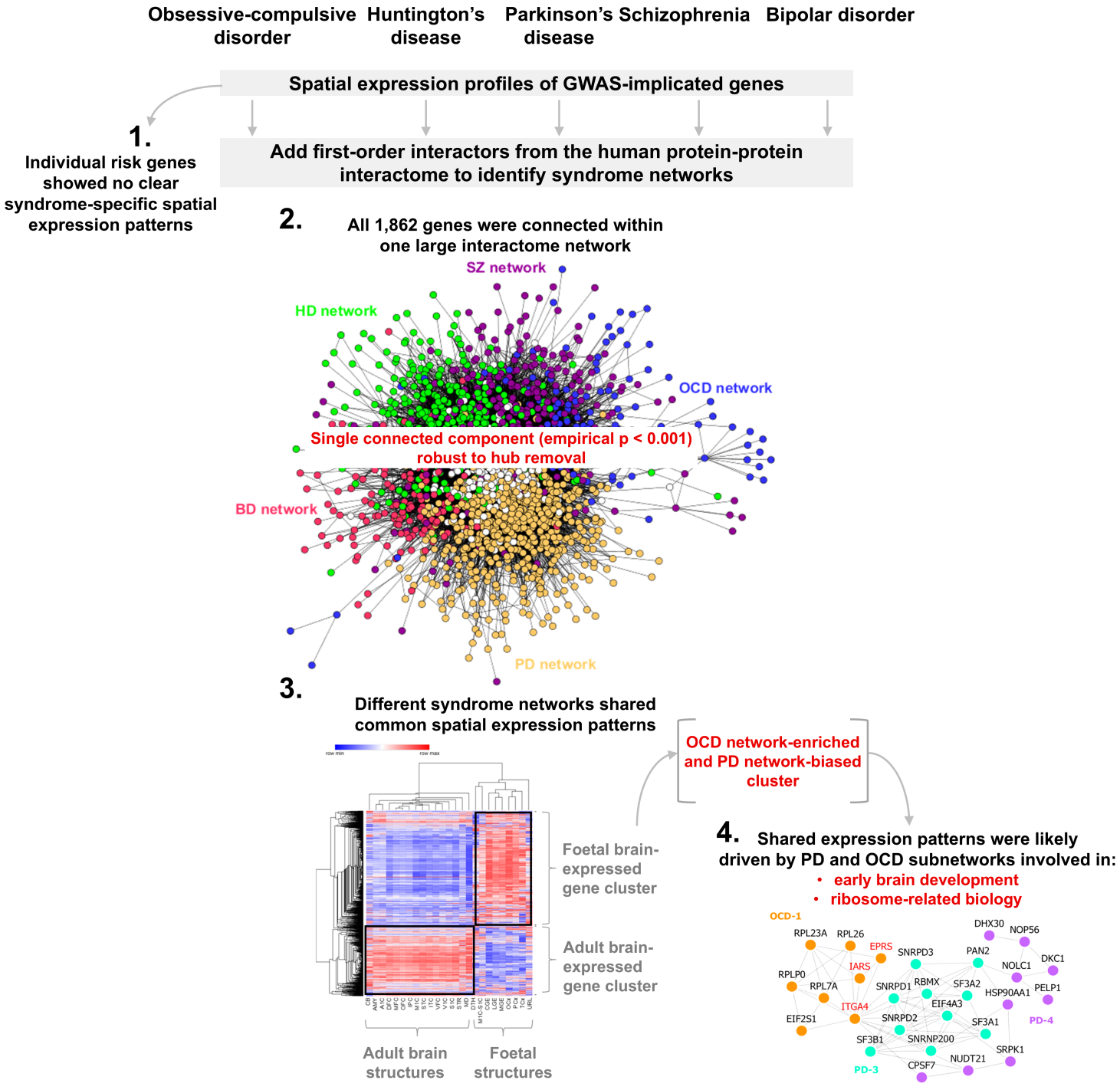


Figure 1

Graphical abstract outlining the analyses conducted in the study. GWAS-implicated genes linked to obsessive-compulsive disorder (OCD), Huntington's disease (HD), Parkinson's disease (PD), schizophrenia (SZ), and bipolar disorder (BD) were collected. The first-order interactors of the proteins encoded by these genes were added using protein-protein interaction (PPI) repositories, BioGRID and HPRD. Degree-preserving PPI enrichment analyses were then conducted to assess the statistical significance of interconnectivity in the resultant network. Next, the spatiotemporal expression profiles of the genes in the combined network were examined to identify clusters with specific regional expression signatures and disorder affiliations. Finally, the network modules contributing to these expression signatures were identified.

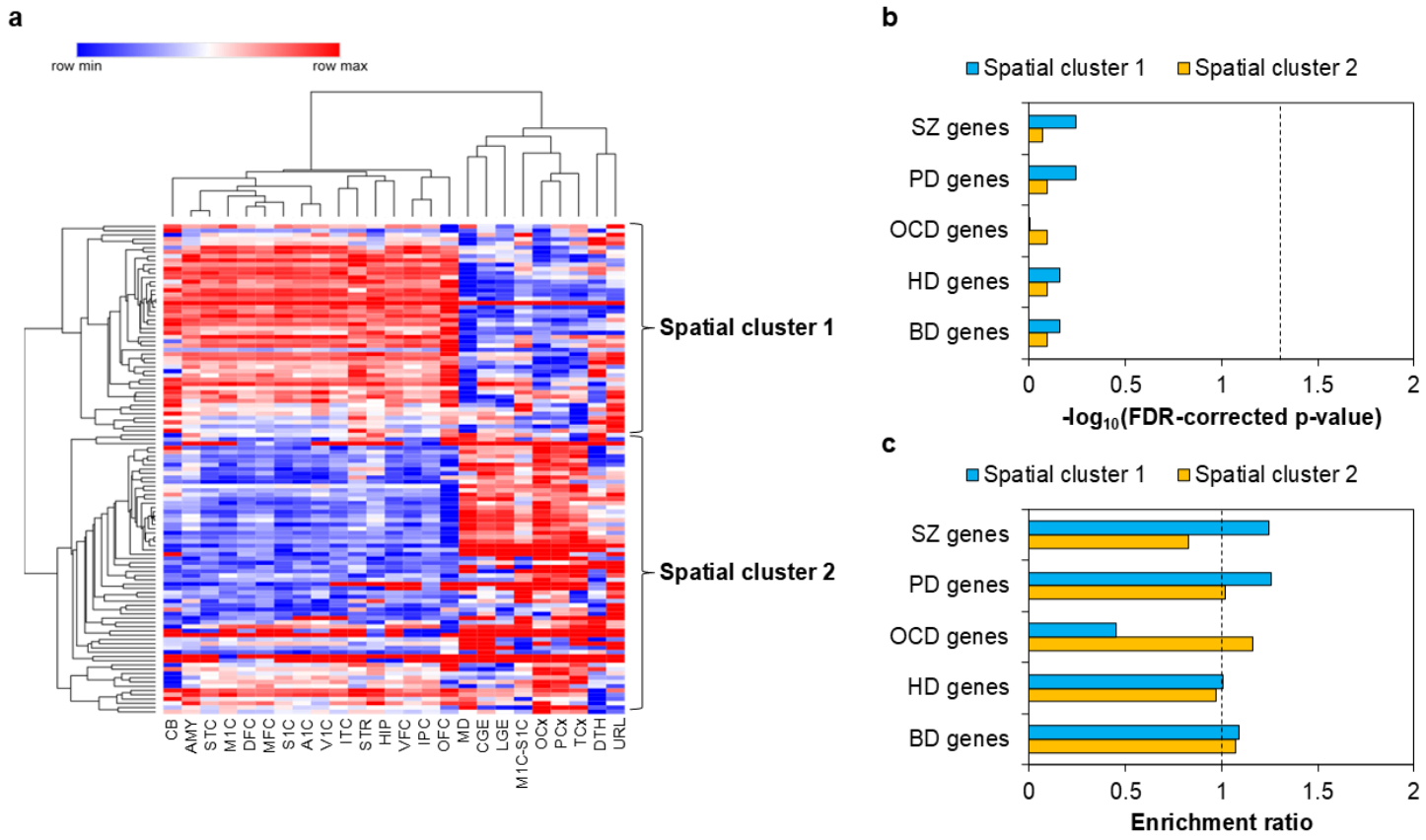


Figure 2

Gene-level spatial clusters fail to capture syndrome affiliations. a Dichotomized average expression of 115 syndrome-associated genes across 524 BrainSpan Atlas samples, spanning 26 brain structures (labelled on bottom horizontal axis). Gene expression across these structures was hierarchically clustered by computing pairwise distances between the data points (log_2-transformed RPKM values) using Pearson correlation, and identifying closely linked clusters using the average linkage method. The clustered heat map was generated using the Morpheus software. **b** Syndrome affiliations of clusters were examined based on statistically significant enrichment of genes associated with specific

syndromes. The dashed black line indicates the significance threshold after Benjamini-Hochberg correction for multiple hypotheses (p-value < 0.05, i.e. $-\log_{10}$(p-value) > 1.30103). **c** Enrichment ratios of clusters for syndrome-specific genes. Ratios indicate the observed frequency of syndrome-associated genes in spatial clusters relative to their expected frequency (based on their distribution in the universal set of genes). The dashed black line indicates the enrichment threshold (ratio > 1).

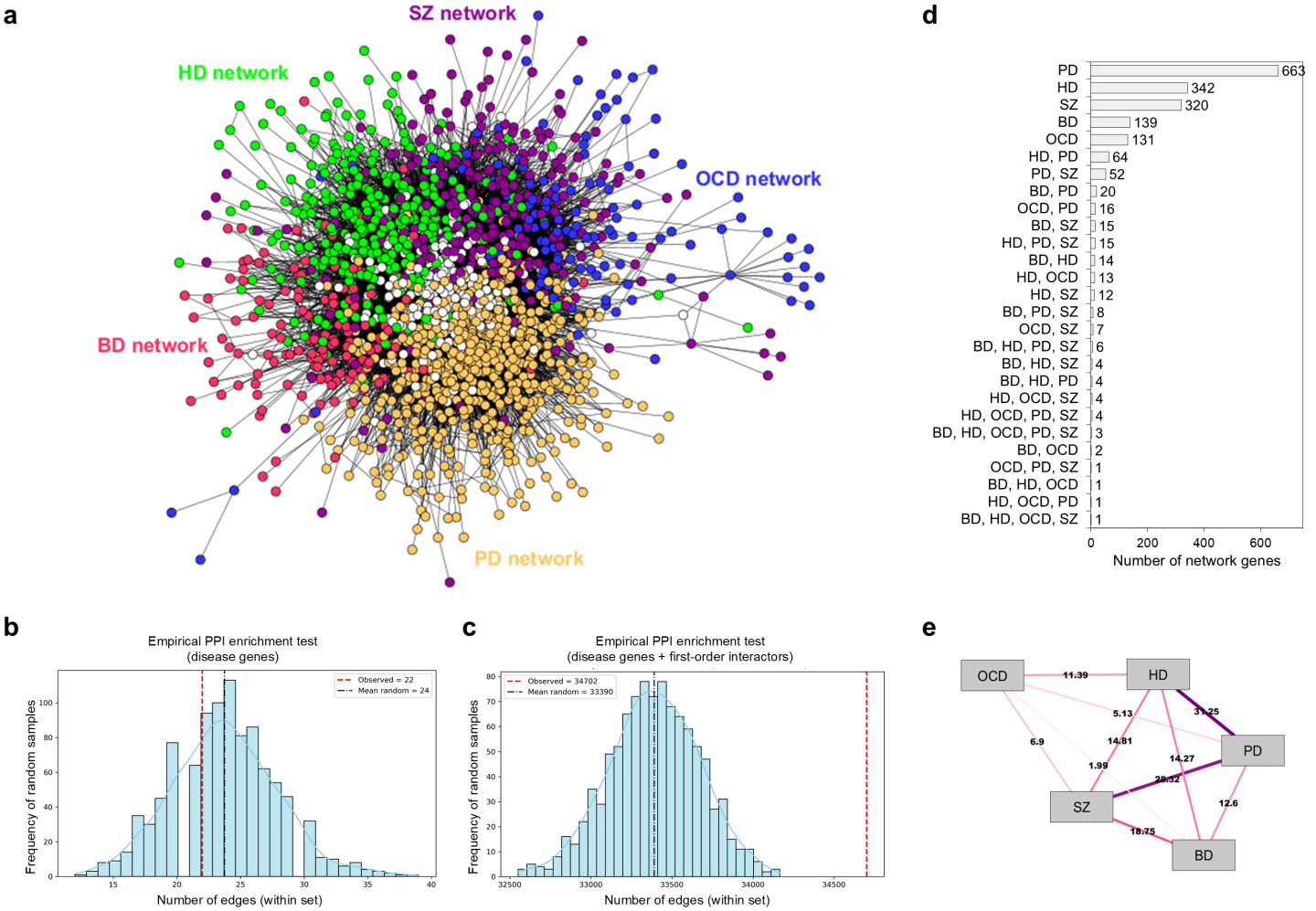


Figure 3

Genes associated with the five syndromes are connected within a single combined protein-protein interaction (PPI) network. a The combined network containing the first-order interactors of genes associated with HD, PD, OCD, SZ, and BD. Genes are shown as nodes and PPIs as edges. Nodes unique to specific syndrome networks are coloured differently, while nodes shared between at least two syndrome networks are shown in white. **b** True number of edges among the disease gene set (red dashed line) and histograms of edge counts from 1,000 degree-matched subsets of the human interactome (mean shown as a black dashed line). **c** True number of edges within the network of disease genes and their first-order interactors (red dashed line) and histograms of edge counts from 1,000 degree-matched subsets from the human interactome (mean shown as a black dashed line). **d** Number

of genes unique to, or shared between, the syndrome networks. **e** Statistical significance of gene sharing between the syndrome networks. The -$\log_{10}$(p-values) of overlaps, indicating the statistical significance of gene sharing between pairs of syndrome networks, are shown next to the edges. Each node represents a syndrome, and each edge represents the pairwise relationship in terms of shared genes. Edge width increases with statistical significance of overlap, and edge colour indicates higher (deeper purple) or lower (lighter purple) levels of statistical significance.

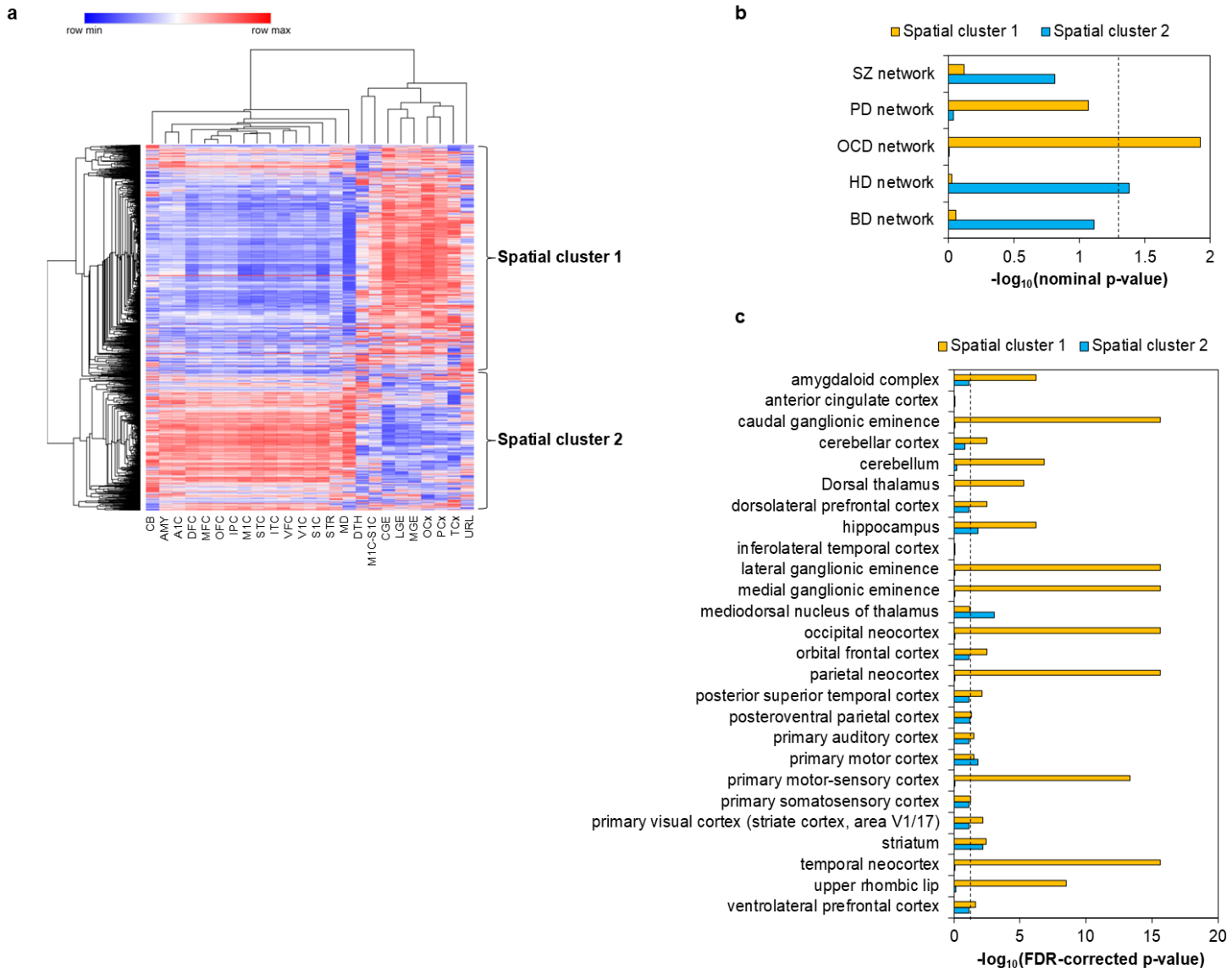


Figure 4

Network-level spatial clusters capture distinct syndrome affiliations and regional specificities. a Dichotomized average expression of 1,826 syndrome network genes across 524 BrainSpan Atlas samples, spanning 26 brain structures (labelled on bottom horizontal axis). Gene expression across these structures was hierarchically clustered by computing pairwise distances between the data points ($\log_2$-transformed RPKM values) using Pearson correlation, and identifying closely linked clusters using the average linkage method. The clustered heat map was generated using the Morpheus software. **b**

Syndrome affiliations of clusters were examined based on statistically significant enrichment of genes belonging to specific syndrome networks. The dashed black line indicates the significance threshold (uncorrected p-value < 0.05, i.e. $-\log_{10}$(p-value) > 1.30103); note that these p-values do not survive FDR correction. **c** Enrichment ratios of clusters for genes with log(RPKM) > 2 in specific brain structures (excluding housekeeping genes with TPM ≥ 1 in the Human Protein Atlas, where TPM is transcripts Per Million). The dashed black line indicates the significance threshold after Benjamini-Hochberg correction for multiple hypotheses (p-value < 0.05, i.e. $-\log_{10}$(p-value) > 1.30103).

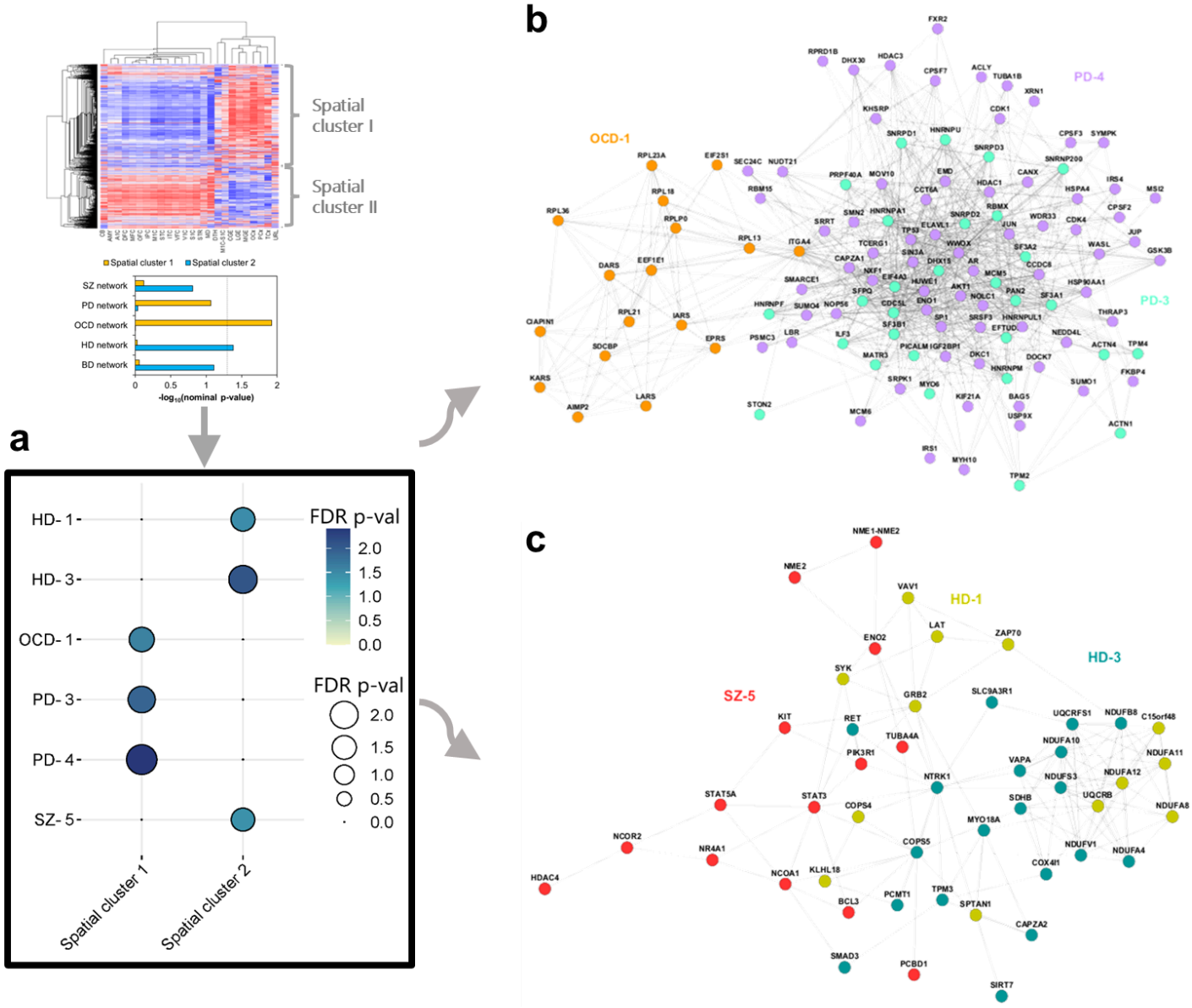


Figure 5

Distinct protein-protein interaction (PPI) modules underlie syndrome-linked spatial signals. a Enrichment of spatial clusters (heat map above reproduced from Fig. 4) for specific syndrome network modules. The balloon plot shows the enrichment of two spatial clusters (X-axis) for genes belonging to

different modules (Y-axis). The size and colour of the circle indicate the FDR-corrected statistical significance of enrichment (shown as -$\log_{10}$(p-value)); larger circles and deeper colours indicate higher statistical significance. **b** Modules identified from spatial cluster 1 and **c** modules from spatial cluster 2 are shown. Network nodes represent proteins, and edges represent PPIs. Nodes belonging to distinct modules are coloured differently.

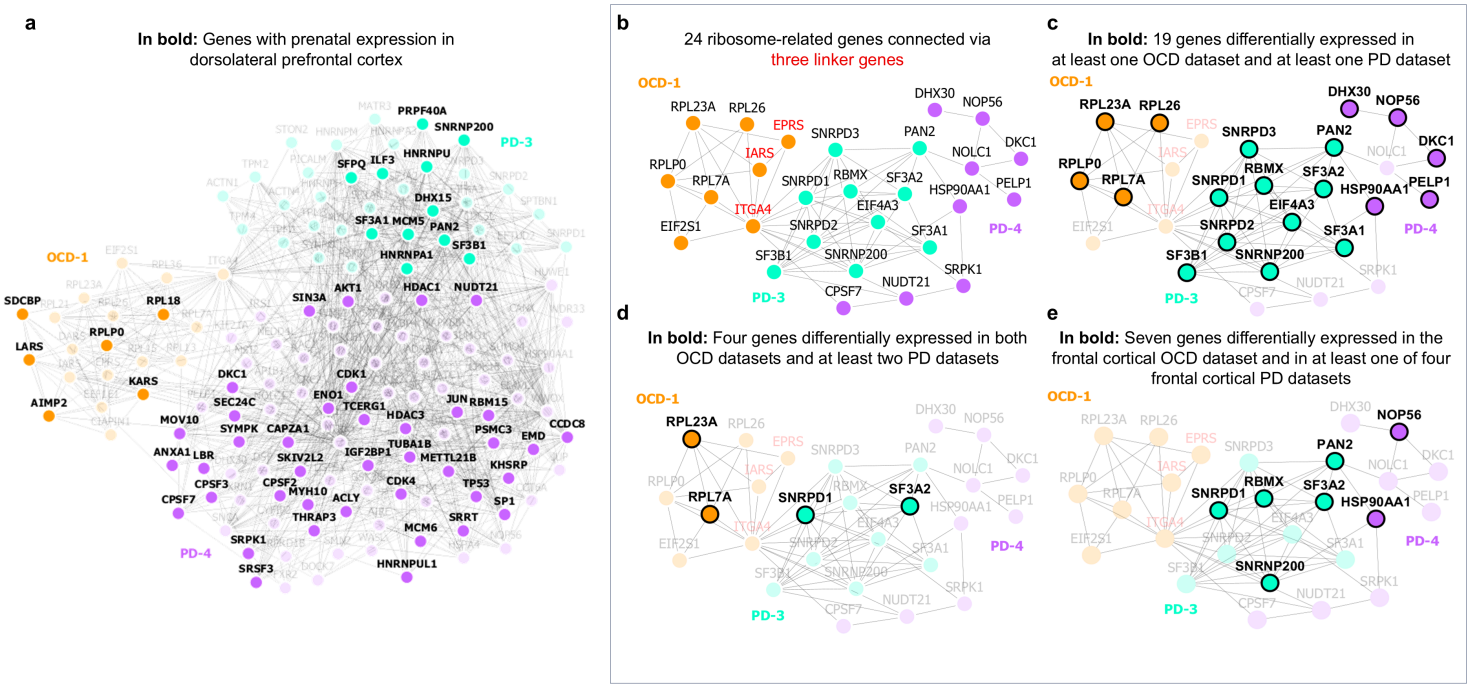


Figure 6

Regional and functional specificities of OCD-1, PD-3 and PD-4 modules. Network nodes represent proteins, and edges represent PPIs. Nodes belonging to distinct modules are coloured differently. OCD and PD modules with **a**genes expressed in prenatal stages of dorsolateral prefrontal cortex development shown in bold, **b** the subnetwork containing 24 ribosome-related genes shown in isolation, and various parts of this subnetwork with evidence for differential expression in OCD and PD datasets highlighted in **c-e**.

Supplementary Files

This is a list of supplementary files associated with this preprint. Click to download.

- npjPDSupplementaryInformationFileFinal.docx
- npjPDSupplementaryDataFilesFinal.xlsx